Article

TRANSPARENT PROCESS

EMBO reports

The thymic cortical epithelium determines the TCR repertoire of IL-17-producing γδT cells

Takeshi Nitta[1], Ryunosuke Muro[1], Yukiko Shimizu[2], Sachiko Nitta[1], Hiroyo Oda[1], Yuki Ohte[3], Motohito Goto[2], Rieko Yanobu-Takanashi[2], Tomoya Narita[4], Hiroshi Takayanagi[4], Hisataka Yasuda[5], Tadashi Okamura[2,6], Shigeo Murata[3] & Harumi Suzuki[1,*]

Abstract

The thymus provides a specialized microenvironment in which distinct subsets of thymic epithelial cells (TECs) support T-cell development. Here, we describe the significance of cortical TECs (cTECs) in T-cell development, using a newly established mouse model of cTEC deficiency. The deficiency of mature cTECs caused a massive loss of thymic cellularity and impaired the development of αβT cells and invariant natural killer T cells. Unexpectedly, the differentiation of certain γδT-cell subpopulations—interleukin-17-producing Vγ4 and Vγ6 cells—was strongly dysregulated, resulting in the perturbation of γδT-mediated inflammatory responses in peripheral tissues. These findings show that cTECs contribute to the shaping of the TCR repertoire, not only of "conventional" αβT cells but also of inflammatory "innate" γδT cells.

Keywords IL-17; thymic epithelial cell; thymus; β5t; γδT
Subject Category Immunology
DOI 10.15252/embr.201540096 | Received 14 January 2015 | Revised 17 February 2015 | Accepted 18 February 2015 | Published online 13 March 2015
EMBO Reports (2015) 16: 638–653

Introduction

The thymic microenvironment is a three-dimensional cellular architecture composed of a set of stromal cells, including thymic epithelial cells (TECs), which guide the development and repertoire formation of T cells [1,2]. In the thymus, there are two anatomically discrete environments, the cortex and medulla, that contain phenotypically and functionally different TEC subsets called cortical TECs (cTECs) and medullary TECs (mTECs), respectively. cTECs form a cortical meshwork densely filled with $CD4^+CD8^+$ (double positive, DP) thymocytes undergoing repertoire selection. Positively selected $CD4^+CD8^-$ (CD4 single positive, CD4SP) and $CD4^-CD8^+$ (CD8SP) thymocytes migrate into the medulla, where mTECs filter out self-reactive SP thymocytes by negative selection. This stepwise developmental process across the distinct microenvironments achieves the development of αβT cells with a diverse yet self-tolerant T-cell receptor (TCR) repertoire.

A series of studies has revealed the importance of mTECs in the establishment of T-cell tolerance. More than 10 strains of mice defective in mTEC development, due to the mutation of cytokines, cytokine receptors, signaling molecules, or transcription factors, have been reported, all of which showed organ-specific, T-cell-dependent autoimmunity [3]. mTECs express a variety of peripheral tissue-specific antigens, at least partly by virtue of the nuclear factor Aire, such that SP thymocytes reactive to self-antigens are deleted [4]. A subset of mTECs produce chemokines CCL19 and CCL21, which attract SP thymocytes from the cortex to the medulla, ensuring deletion of self-reactive cells [5]. Studies with mTEC-deficient mice revealed that mTECs are also required for development of regulatory T cells (Tregs) [6] and maturation of invariant natural killer T (iNKT) cells [7].

On the other hand, the thymic cortex has been studied mainly as a place for positive selection of αβT cells owing to the unique proteolytic and antigen processing capabilities of cTECs that are essential for positive selection. A proteasome subunit β5t, which is specifically expressed in cTECs [8,9], regulates positive selection of CD8 T cells by producing unique MHC class I-bound peptides in cTECs [10,11]. Furthermore, cTECs highly produce endosomal/lysosomal proteases, cathepsin L [12] and thymus-specific serine protease [13], which contribute to the generation of MHC class II-bound peptides and positive selection of certain repertoire of CD4 T cells. However, when compared with mTECs, the physiological significance of cTECs has been less addressed, partly because of a few reports on cTEC-deficient mice [14,15]. Thus, whether and how cTECs contribute to the development and function of the immune system, other than in the context of positive selection of αβT cells, remains to be elucidated.

In addition to the conventional and unconventional αβT-cell lineages described above, the thymus also supports the development

1 Department of Immunology and Pathology, Research Institute, National Center for Global Health and Medicine, Chiba, Japan
2 Department of Laboratory Animal Medicine, Research Institute, National Center for Global Health and Medicine, Tokyo, Japan
3 Laboratory of Protein Metabolism, Graduate School of Pharmaceutical Sciences, The University of Tokyo, Tokyo, Japan
4 Department of Immunology, Graduate School of Medicine and Faculty of Medicine, The University of Tokyo, Tokyo, Japan
5 Bioindustry Division, Oriental Yeast Co., Ltd., Tokyo, Japan
6 Section of Animal Models, Department of Infectious Diseases, Research Institute, National Center for Global Health and Medicine, Tokyo, Japan
*Corresponding author. Tel: +81 47 373 5539; Fax: +81 47 372 5539; E-mail: hsuzuki@ri.ncgm.go.jp

of γδT cells [16]. In fact, development of $V\gamma5^+$ γδT cells was shown to be dependent on Skint1 expressed on mTECs [17]. Recent studies have paid particular attention to a subpopulation of γδT cells as an important source of interleukin (IL)-17 in various infections or inflammatory disorders [18–20], although regulation of the development of IL-17-producing γδT cells in the thymus remains largely unclear.

In the present study, we describe a novel mutant mouse strain harboring a spontaneous point mutation resulting in substantial loss of mature cTECs. We utilized these mice to study the significance of cTECs in T-cell development *in vivo*. Our results demonstrated that cTECs are required for the increase in thymic volume and optimum development of conventional αβT cells and iNKT cells. We also found that cTECs control the TCR repertoire of IL-17-producing γδT cells and thereby contribute to γδT cell-dependent inflammatory responses.

Results

Thymic hypoplasia and impaired thymocyte development in *TN* mice

A spontaneous mutant mouse line that exhibited a T lymphopenia was found in our in-house breeding colony of C57BL/6 mice. These mice showed a significant reduction of $CD3^+CD44^{lo}$ naïve T cells in peripheral blood (Fig 1A), with no apparent defects in growth or reproduction. We named this mouse strain "*T lymphopenia of naïve population* (*TN*)". After several generations of in- and outbreeding, we found that heterozygous mutant mice (+/*tn*) showed a mild reduction of naïve T cells (25.7% of wild-type) and homozygous mutant mice (*tn*/*tn*) showed a severe naïve T-cell reduction (6.0% of wild-type). Mating tests indicated that the T lymphopenia was inherited as an autosomal dominant trait (Supplementary Fig S1).

Compared with wild-type, *TN* mice had strikingly smaller thymi and markedly reduced numbers of total thymocytes (Fig 1B and C). The frequency of CD4SP and CD8SP mature thymocytes was significantly reduced in *TN* mice (Fig 1D and E), whereas the frequency of DP thymocytes was unchanged. Bone marrow cells from *tn*/*tn* mice readily reconstituted thymocyte development in irradiated wild-type mice, whereas +/*tn* and *tn*/*tn* host mice did not support thymocyte development of wild-type bone marrow cells (Supplementary Fig S2), indicating that non-hematopoietic stromal cells, likely thymic stromal cells, are responsible for the impaired T-cell development in *TN* mice.

TN mice lack mature cTECs

In the thymus from *tn*/*tn* mice, the contrast and boundary between cortex (wherein DP thymocytes localize) and medulla (wherein CD4SP and CD8SP thymocytes localize) were clearly detectable as seen in wild-type thymus (Fig 2A). However, the expression of cTEC markers such as CD205, Ly51, and keratin 8 was almost undetectable in *tn*/*tn* thymus, whereas mTEC markers such as UEA1, keratin 5, Aire, and CCL21 were detectable (Fig 2A and Supplementary Fig S3A). The *tn*/*tn* cortex that hosted DP thymocytes was composed of $keratin^+$ TECs without expression of cTEC and mTEC markers (likely immature TECs as described later). Electron microscopy showed that the cortical epithelial network that was characteristic in wild-type thymus was poorly developed in *tn*/*tn* thymus (Fig 2B). Flow cytometric analysis of collagenase-digested thymic stromal cells from adult mice confirmed the nearly complete loss of $CD205^{hi}UEA1^-$ cTECs in *tn*/*tn* mice (Fig 2C). During thymic ontogeny in wild-type mice, $CD205^{hi}UEA1^-$ cTECs were detected by embryonic day (E) 16.5 and their number increased exponentially until birth and was maintained in postnatal thymus until young adult age. However, this same cTEC population was negligible throughout embryogenesis and postnatal development in *tn*/*tn* mice (Fig 2D and Supplementary Fig S3C). Development of cTECs also failed in *in vitro* organ culture of E14.5 fetal thymus, indicating that this defect was thymus-intrinsic (Supplementary Fig S3D).

In the postnatal thymus from *tn*/*tn* mice, the frequency of $CD205^{lo}UEA1^+$ mTECs was partially reduced (Fig 2C and D). Despite the reduced frequency of mTECs in *tn*/*tn* mice, treatment with RANKL, an mTEC-promoting cytokine [21], successfully induced expansion of mTECs in organ culture of *tn*/*tn* thymus (Supplementary Fig S3E), indicating that the developmental potential of mTECs was not aberrant in *tn*/*tn* mice.

The most prominent population of TECs from *tn*/*tn* mice was $CD205^{lo}UEA1^-$ cells that showed low surface expression of MHC class II (Supplementary Fig S3F). As the expression of MHC class II gradually increases along the maturation process of TECs [9,22], our results indicate that $CD205^{lo}UEA1^-$ cells in *tn*/*tn* mice are immature TECs. Expression of cTEC-associated genes, including *CtsL*, *Psmb11*, *Prss16*, *Il7*, *Dll4*, and *Cxcl12*, was detected at low levels in $CD205^{lo}UEA1^-$ TECs from *tn*/*tn* mice, while mTEC-associated genes, including *CtsS*, *Aire*, and *Skint1*, were almost undetectable (Fig 3E). These results, along with recent reports that cTECs and mTECs are derived from TEC progenitors expressing cTEC-associated genes [23–25], indicate that $CD205^{lo}UEA1^-$ TECs that reside in the thymic cortex of *tn*/*tn* mice are immature TEC progenitors and that *tn*/*tn* mice are defective in the generation of mature cTECs from immature TEC progenitors.

A missense mutation of β5t impairs cTEC development

By linkage analysis followed by deep sequencing of the entire 11-Mb candidate region on chromosome 14, we identified a homozygous missense mutation in *tn*/*tn* mice in the *Psmb11* gene, the gene that encodes the cTEC-specific proteasome subunit β5t (Fig 3A). This mutation is a G to A nucleotide substitution, which causes a Gly 220 to Arg codon change (G220R) in β5t (Fig 3B). To confirm that the $Psmb11^{G220R}$ mutation was primarily responsible for the *TN* phenotypes, we performed CRISPR/Cas9-mediated genome editing in mice. Targeted disruption of the $Psmb11^{G220R}$ allele or single nucleotide reversion from $Psmb11^{G220R}$ to $Psmb11^{WT}$ in +/*tn* mice completely restored thymocyte cellularity and development of mature cTECs up to wild-type levels (Fig 3C–E). These results clearly indicate that the $Psmb11^{G220R}$ is the causative mutation responsible for the *TN* phenotype.

β5t is a proteasome subunit exclusively expressed in cTECs that forms an atypical type of proteasome, termed the "thymoproteasome" [8,9], that is required for positive selection of $CD8^+$ T cells [10,11]. It was quite unexpected that the single amino acid substitution of β5t could account for such severe defects, because mice lacking β5t showed normal cTEC development by the redundant

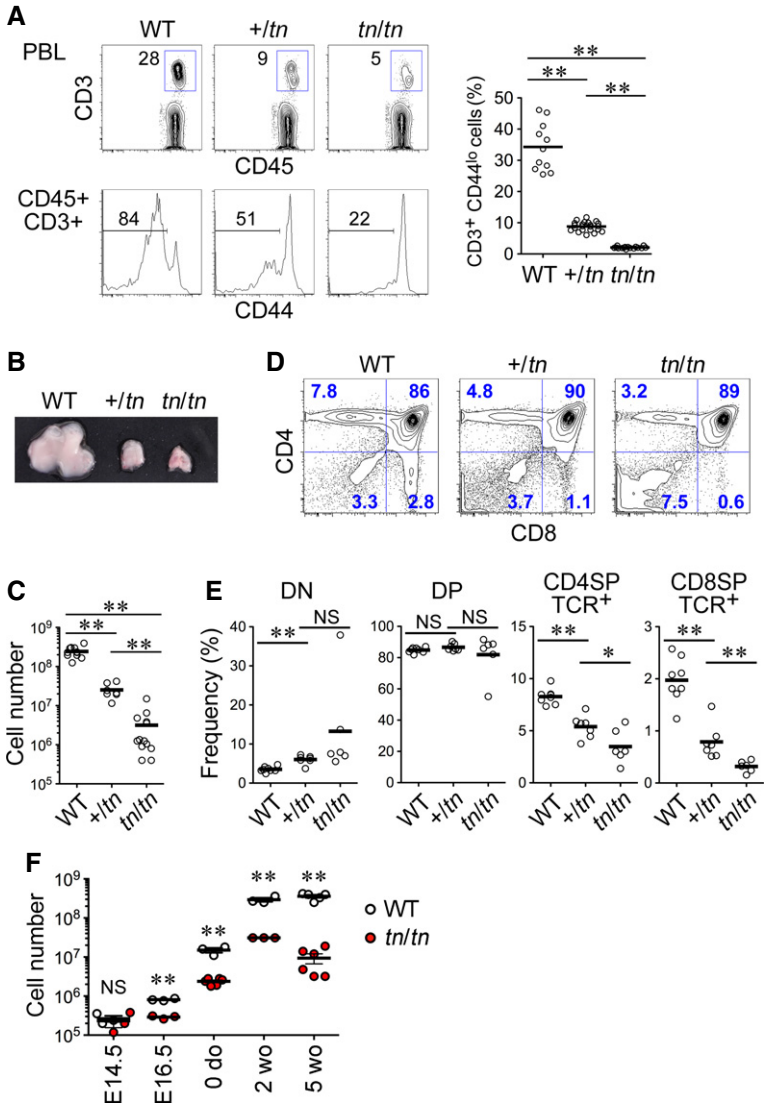

Figure 1. Thymus hypoplasia and impaired T-cell development in *TN* mice.

A Frequency of naïve T cells in peripheral blood leukocytes (PBL). PBL from wild-type (WT) (n = 11), +/*tn* (n = 22), or *tn*/*tn* (n = 16) mice were analyzed by flow cytometry for CD45, CD3ε, and CD44 (left). Numbers indicate percentage of cells within indicated areas. Graph indicates percentages of $CD3^+CD44^{lo}$ naïve T cells in total $CD45^+$ leukocytes (right).

B Representative photograph of thymi from 5-week-old mice.

C Total numbers of thymocytes from 5-week-old mice (n = 7–13).

D Flow cytometry profiles for CD4 and CD8 of total thymocytes from 5-week-old mice.

E Frequency of indicated thymocyte populations.

F Numbers of whole thymic cells prepared from indicated ages of WT (n = 3–5) or *tn*/*tn* (n = 3–6) mice.

Data information: Data represent more than three independent experiments. Each circle represents an individual mouse, and horizontal bars indicate the mean. The statistical significance between indicated groups was calculated with an unpaired one-tailed Student's t-test. *$P < 0.05$; **$P < 0.01$; NS, not significant.

complementation with another subunit β5i [10,11]. Along with the fact that heterozygous +/*tn* mice also exhibited the *TN* phenotype, it is evident that the G220R mutation of β5t has a dominant-negative effect, instead of a loss-of-function effect. To examine the effect of the G220R mutant on thymoproteasomes containing β5t, β1i, and β2i subunits, we utilized retroviral expression of β5t in β5i-deficient ($\beta5i^{-/-}$) mouse embryonic fibroblast (MEF) cells, wherein β1i and β2i could be induced by interferon-γ (IFNγ) stimulation. The mutant $\beta5t^{G220R}$ protein was not proteolytically processed to its mature form (Fig 4A), nor was it assembled with other subunits (Fig 4B). Its expression resulted in the accumulation of proteasome assembly intermediates (Fig 4C), and correlated with reduced amounts of mature β1i and β2i subunits (Fig 4A) and of total 20S proteasomes (Fig 4D). These results indicate that the $\beta5t^{G220R}$ mutant protein disturbs normal proteasome assembly in cTECs. In fact, impaired thymoproteasome assembly was observed *in vivo* in fetal thymus

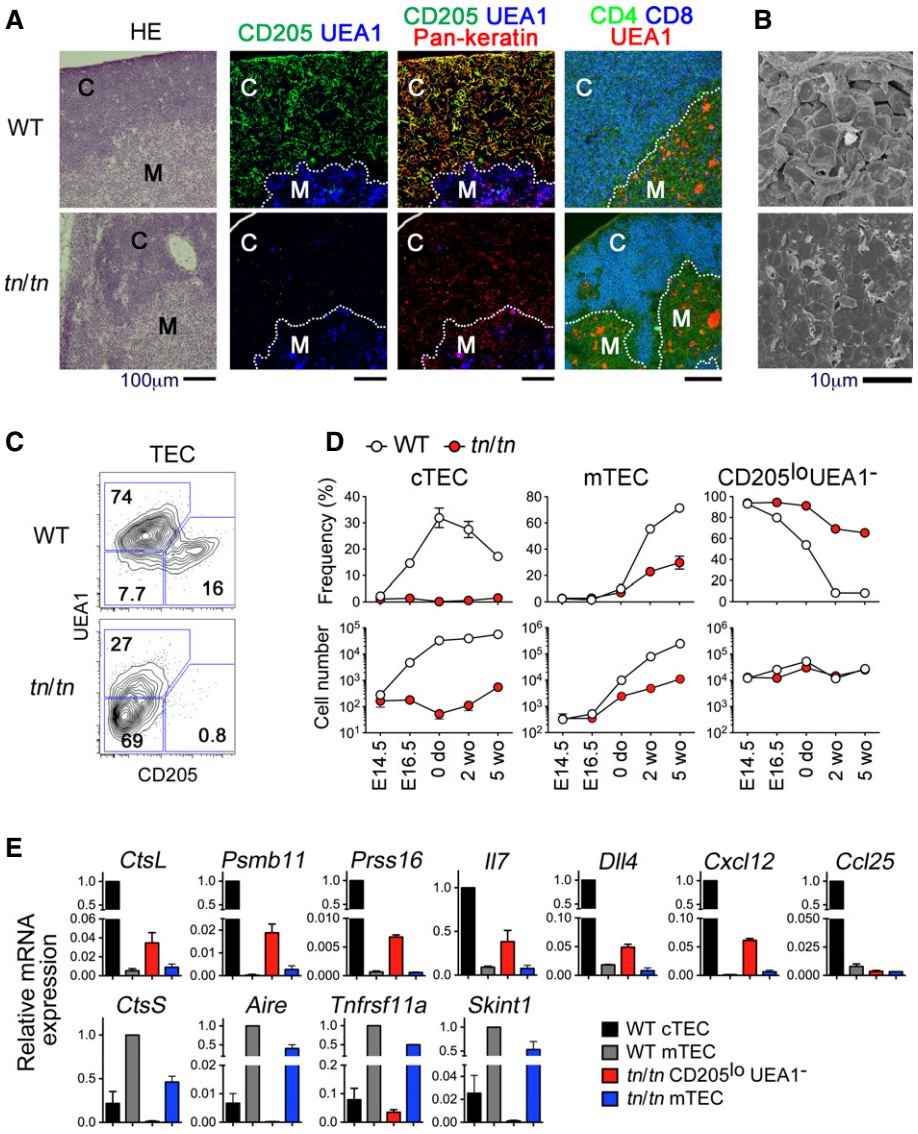

Figure 2. *TN* mice lack mature cTECs.

A Thymus sections from 5-week-old WT or *tn/tn* mice were stained with hematoxylin and eosin (HE), or for CD205, UEA1, pan-keratin, CD4, and CD8. "C" denotes cortex and "M" denotes medulla. Dotted lines indicate cortex/medulla boundary. Scale bars indicate 100 μm.

B Scanning electron micrographs of thymic cortex from WT or *tn/tn* mice. Scale bar indicates 10 μm.

C Flow cytometry profiles for CD205 and UEA1 of EpCAM$^+$Keratin$^+$ TECs prepared from 5-week-old WT or *tn/tn* mice.

D Frequency (% of EpCAM$^+$Keratin$^+$ cells) (top) and numbers (per mouse) (bottom) of CD205^{hi}UEA1$^-$ (cTEC), CD205^{lo}UEA1$^+$ (mTEC), or CD205^{lo}UEA1$^-$ TECs from the indicated ages of WT or *tn/tn* mice (n = 3–5, mean ± SEM).

E Quantitative RT–PCR analysis of the indicated genes in isolated TECs (n = 3, mean ± SE). mRNA expression was normalized to EpCAM mRNA, and those in WT cTECs or WT mTECs were arbitrarily set to 1.

Data information: Data represent more than three independent experiments (A, C, D, E) or one experiment with three mice per group (B).

from *tn/tn* mice (Fig 4E). Consistent with an absolute requirement of proteasome activity for cell survival [26,27], exogenous expression of β5t^{G220R} induced cell death in different cell types in a dose-dependent manner (Fig 4F and G). Indeed, in *tn/tn* neonatal thymus, mature β5t^{hi} cTECs were specifically absent, while immature β5t$^{med/lo}$ TEC populations remained (Fig 4H). Finally, residual cTECs in fetal thymus from *tn/tn* mice exhibited higher accumulation of polyubiquitinated proteins and a higher occurrence of cell death than those from wild-type mice (Fig 4I). Collectively, we concluded that β5t^{G220R} mutant protein inhibits normal proteasome assembly and thus induces cell death in mature cTECs that highly express β5t. The moderate defects of mTECs in *tn/tn* mice may be due to an effect of low level expression of β5t^{G220R} on bipotent TEC progenitors and a reduction of SP thymocytes that provide RANKL. Thus, *TN* mice represent a β5t-driven, novel mouse model of cTEC deficiency.

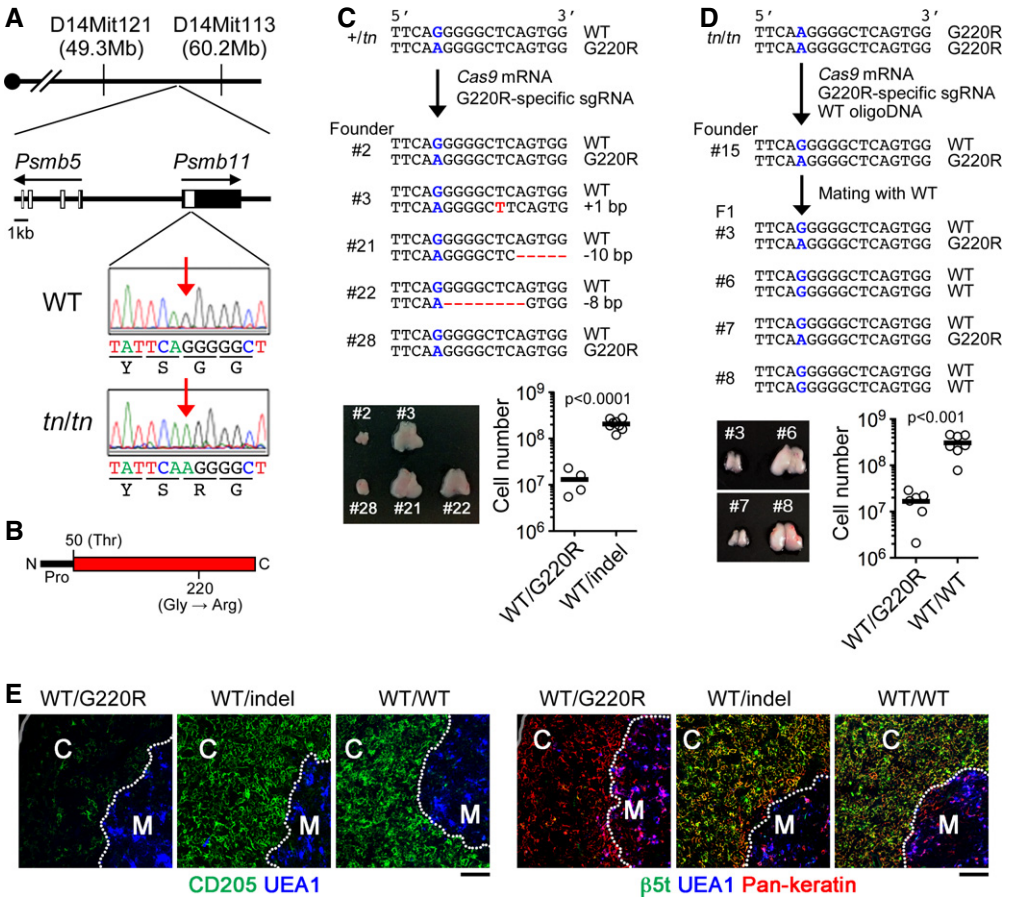

Figure 3. A missense mutation of the *Psmb11* gene causes cTEC deficiency in *TN* mice.

A Genetic map of the *tn* locus on chromosome 14 and representative sequencing results of *Psmb11* from WT or *tn/tn* mice. Red arrows indicate the position of the mutation.

B The structure of the β5t protein. The positions of N-terminal propeptide (Pro), catalytically active site (Thr50), and G220R mutation are shown.

C, D *Cas9* mRNA and *Psmb11*^{G220R}-specific single-guide (sg) RNA were injected into +/*tn* fertilized eggs, and generated founder mice were genotyped and analyzed (C). *Cas9* mRNA, *Psmb11*^{G220R}-specific sgRNA, and WT oligonucleotide were injected into *tn/tn* fertilized eggs, and a generated founder mouse (#15) was crossed with WT mice (D). The sequences of both alleles of *Psmb11* in representative mice are shown (top). G220R mutation site is labeled in blue. Insertion and deletion (indels) are labeled in red. Representative photographs of thymi and total numbers of thymocytes from mice of the indicated genotype are shown (bottom). Each circle represents an individual mouse, and horizontal bars indicate the mean. The statistical significance was calculated with an unpaired one-tailed Student's *t*-test.

E Thymus sections from mice with the indicated *Psmb11* genotypes (see C, D) were stained for CD205, UEA1, β5t, and pan-keratin. Scale bars indicate 100 μm. "C" denotes cortex and "M" denotes medulla. Dotted lines indicate cortex/medulla boundary.

Data information: Data represent more than three (C, D) or two (E) experiment(s).

Impaired αβT-cell development in *TN* mice

The findings described above prompted us to utilize *TN* mice to study the significance of cTECs in T-cell development and the immune system *in vivo*. First, we observed that thymic cellularity was associated with the expansion of mature cTECs during ontogeny. In E14.5 fetal thymus, there were no differences in thymic cellularity (Fig 1F) or epithelial architecture (Supplementary Fig S3B) between wild-type and *tn/tn* mice. After E16.5, *tn/tn* mice exhibited reduced thymic cellularity, which coincided with the impaired maturation of cTECs (Fig 2D). These results indicate the requirement of mature cTECs for maximizing the size of the thymus.

We next examined αβT-cell development. Among CD4$^-$CD8$^-$ (double negative, DN) thymocytes, the proportion of c-Kit$^+$CD25$^-$ (DN1) and c-Kit$^+$CD25$^+$ (DN2) cells was significantly reduced in postnatal *tn/tn* mice (Fig 5A). *tn/tn* mice also showed a markedly reduced frequency of c-Kit$^-$CD25$^+$CD27^{hi} (DN3b) cells, which represent post-β-selection DN3 thymocytes, whereas c-Kit$^-$CD25$^+$CD27^{lo} (DN3a) and c-Kit$^-$CD25$^-$ (DN4) cells were unaffected. These results indicate that optimal development of DN thymocytes requires mature cTECs.

In mice expressing either polyclonal or monoclonal TCRs (OT-I and OT-II), TCRβ^{hi}CD69$^+$ post-selected DP thymocytes and CD4SP or CD8SP thymocytes were markedly reduced, indicating that positive selection of αβT cells was impaired in *tn/tn* mice (Fig 5B–D). The αβT cells that developed in *tn/tn* mice carried an altered TCR repertoire, as the distribution of TCR-Vα and TCR-Vβ in splenic T cells and SP thymocytes was significantly different between wild-type and *tn/tn* mice (Fig 5E). By contrast, negative selection mediated by mammary tumor virus (*mtv*)-encoded superantigen

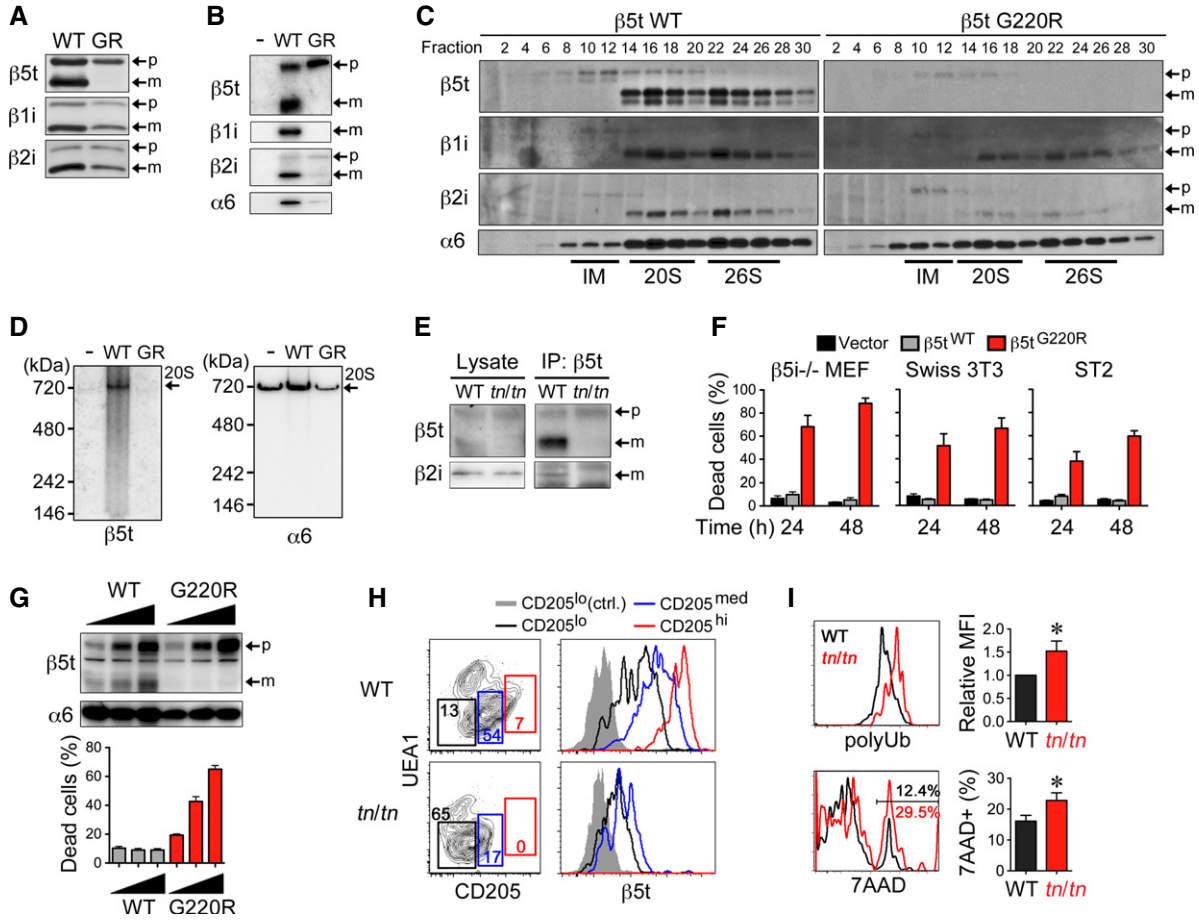

Figure 4. β5t^{G220R} impairs proteasome assembly and cell survival in cTECs.

A–D β5i$^{-/-}$ mouse embryonic fibroblasts (MEFs) were infected with retroviruses expressing C-terminally FLAG-tagged β5t^{WT} or β5t^{G220R} (GR) and treated with IFNγ. Forty hours after infection, total cell lysates (A) and immunoprecipitates with anti-FLAG antibody (B) were analyzed by immunoblotting. Cell lysates were fractionated by glycerol density gradient, and each fraction was used for immunoblotting and measurement of chymotrypsin-like proteasomal activity (C). Fractions 8–12, 14–18, and 22–26 contained assembly intermediates (IM), 20S proteasomes, and 26S proteasomes, respectively. Cell lysates were subjected to native PAGE followed by immunoblotting (D). Arrows indicate precursor (p) and mature (m) forms of β-subunits (A–C) or 20S proteasomes (20S) (D).

E Cell lysates from E15.5 fetal thymus were immunoprecipitated with anti-β5t antibody followed by immunoblotting for β5t and β2i.

F β5i$^{-/-}$ MEFs, Swiss 3T3 fibroblast cells, and ST2 bone marrow stromal cells were infected with retroviruses expressing β5t^{WT} or β5t^{G220R} or with empty retroviruses (Vector). β5i$^{-/-}$ MEFs were treated with IFNγ. Thirty hours after infection, EGFP^{+} cells were sorted and re-plated for additional culture for 24 or 48 h. Cells were detached and their viability was assessed by the trypan blue exclusion method (n = 3).

G β5i$^{-/-}$ MEFs were retrovirally infected and treated with IFNγ. Thirty hours after infection, EGFP^{lo}, EGFP^{med}, and EGFP^{hi} cells were sorted and then immunoblotted for expression of β5t and α6 or re-plated for additional 24-h culture. Cell viability was assessed by the trypan blue exclusion method (n = 3).

H Flow cytometry profiles for CD205 and UEA1 of gated EpCAM^{+}Keratin^{+} TECs prepared from 1-week-old mice (left). Numbers indicate percentage of cells within indicated areas. Histograms show intracellular β5t expression in CD205^{lo} (black), CD205^{med} (blue), and CD205^{hi} (red) cells and control staining of CD205^{lo} cells (gray shaded).

I Gated CD205$^{med/hi}$UEA1^{-} cTECs from E16.5 fetal thymus were further analyzed for cellular accumulation of polyubiquitinated proteins (polyUb) (top) and dead-cell staining by 7-aminoactinomycin D (7AAD) (bottom). Graphs show polyUb mean fluorescence intensity (MFI) and frequency of 7AAD^{+} dead cells (n = 3–5). The statistical significance was calculated with an unpaired one-tailed Student's t-test. *P < 0.05.

Data information: Data represent three (A–F, I) or two (G, H) independent experiments (error bars, SEM).

was not affected in *tn/tn* mice (Fig 5F). These results indicate that mature cTECs are required for positive selection and repertoire formation, but dispensable for negative selection, of αβT cells, which is consistent with previous findings [10,11].

Reduced development of iNKT cells in *TN* mice

We then asked whether the cTEC deficiency influenced the development of unconventional αβT-cell lineages such as iNKT cells, Foxp3^{+} Tregs, and CD8αα^{+} TCRαβ intraepithelial lymphocytes (IELs), all of which develop from cortical DP thymocytes. We found a significant reduction of iNKT cells that are reactive to CD1d tetramer loaded with α-galactosylceramide (αGalCer) in the thymus, liver, and spleen from *tn/tn* mice (Fig 6A and B). The ratio of thymic iNKT to DP cells was markedly reduced in *tn/tn* mice, indicating that development of iNKT cells from DP thymocytes is impaired in the absence of mature cTECs (Fig 6C). iNKT cell development depends on positive selection by CD1d/glycolipid

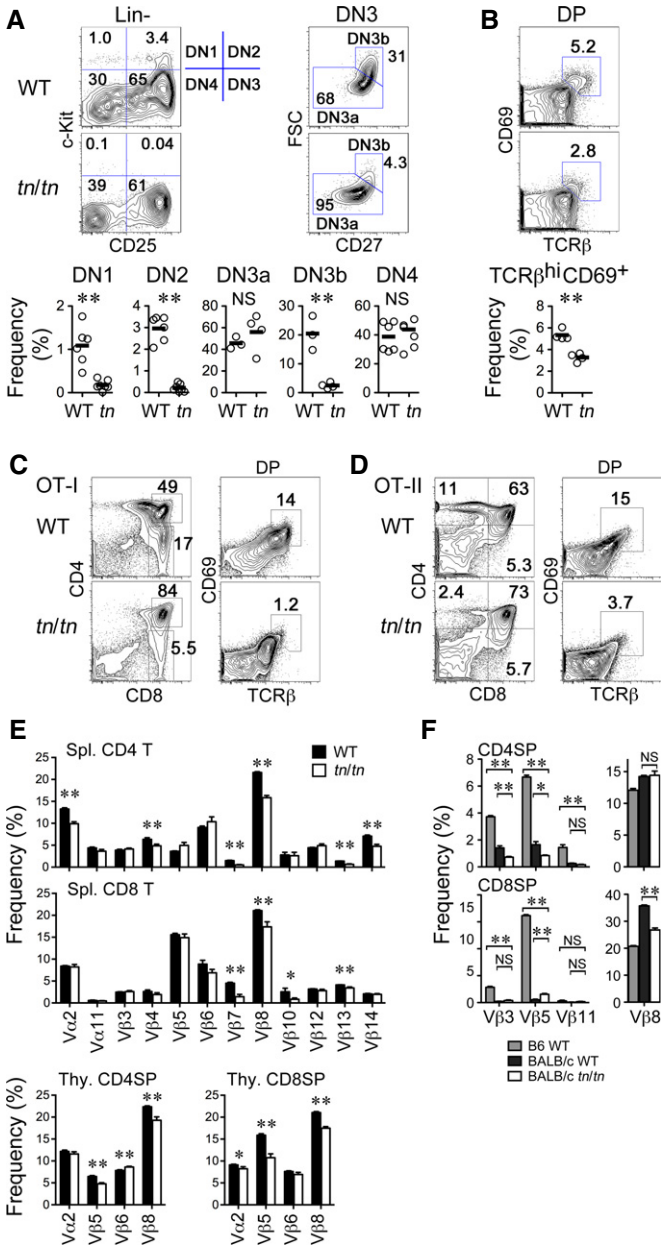

Figure 5. Impaired development of conventional αβT cells in *TN* mice.
Thymocytes from 5-week-old mice were analyzed by flow cytometry.

A Flow cytometry profiles of gated Lin$^-$ (CD3$^-$CD4$^-$CD8$^-$CD11b$^-$CD11c$^-$CD19$^-$NK1.1$^-$) or DN3 (Lin$^-$c-Kit$^-$CD25$^+$) thymocytes (top) and frequency of DN1 (c-Kit$^+$CD25$^-$), DN2 (c-Kit$^+$CD25$^+$), DN3a (c-Kit$^-$CD25$^+$CD27^{lo}FSC^{lo}), DN3b (c-Kit$^-$CD25$^+$CD27^{hi}FSC^{hi}), or DN4 (c-Kit$^-$CD25$^-$) populations (bottom) (n = 4–6) are shown.

B TCRβ and CD69 expression profiles of DP (CD4$^+$CD8$^+$) thymocytes (top) and their frequency (bottom) (n = 4).

C, D Flow cytometry profiles of total and gated thymocytes from OT-I (C) or OT-II TCR transgenic (D) mice.

E Distribution of TCR-Vα and TCR-Vβ in spleen CD4 T or CD8 T cells or CD4SP or CD8SP thymocytes (n = 6–12).

F Distribution of TCR-Vβ3, TCR-Vβ5, TCR-Vβ11, and TCR-Vβ8 in CD4SP or CD8SP thymocytes from WT mice of C57BL/6 (B6) background (n = 2–5) and WT (n = 3–4) or *tn/tn* mice (n = 3–4) of BALB/c background.

Data information: Each circle represents an individual mouse, and horizontal bars indicate the mean (A, B). Mean ± SEM (E, F). *P < 0.05; **P < 0.01; NS, not significant (unpaired t-test). Data in (F) were analyzed by one-way ANOVA. Data represent more than three independent experiments.

complexes expressed on the surface of other DP thymocytes [28]. However, no significant reduction was observed in either CD1d expression or TCR-Vα14-Jα18 rearrangement in DP thymocytes from *tn/tn* mice (Fig 6D and E), suggesting the possibility that the reduced development of iNKT cells is due to impaired interaction between CD1d-expressing "selector" DP thymocytes and TCR-Vα14-Jα18-expressing "iNKT precursor" DP thymocytes. It could be an effect of the marked reduction of absolute numbers of DP thymocytes in *tn/tn* thymus. It is also possible that the cTEC-dependent cortical epithelial network is important for optimal cell–cell contact among DP thymocytes, thereby supporting positive selection of iNKT cells. iNKT cells from *tn/tn* thymus normally expressed TCR-Vβ2, TCR-Vβ7, or TCR-Vβ8 (Fig 6F), indicating that the TCR repertoire of iNKT cells was unaffected by cTEC deficiency. The majority of iNKT cells from *tn/tn* thymus were mature CD44$^+$NK1.1$^+$ (stage 3) cells (Fig 6G), but the frequency of CD44$^+$NK1.1$^-$ (stage 2) cells was significantly reduced. Intracellular staining for key transcription factors revealed that PLZF$^+$ NKT2 cells, but not RORγt$^+$ NKT17 cells, were markedly (P < 0.01) reduced (Fig 6H). Reduction of stage 2 iNKT cells could be due to the reduction of NKT2 cells, because most of the NKT2 cell falls into stage 2 [29]. Although further analysis of the molecular mechanisms of cTEC-mediated selection and differentiation, as well as mTEC-mediated maturation [7], of iNKT cells should be required, our present finding that differential requirement of cTEC for the differentiation of NKT2 and NKT17 cells is intriguing.

The frequency of Foxp3$^+$CD25$^+$ Tregs in CD4SP thymocytes and their distribution in the thymic medulla were similar between wild-type and *tn/tn* mice (Supplementary Fig S4A and B). We also found no significant reduction in the frequencies of TCRβ$^+$CD5$^+$ thymic CD8αα$^+$ IEL precursors or IEL subpopulations, including CD8αα$^+$ TCRαβ IELs, isolated from small intestine (Supplementary Fig S4C and D). These results indicate that the thymic development of Tregs and IELs does not require mature cTECs.

Altered γδT17 cell repertoire in *TN* mice

Lastly, we addressed γδT-cell development in *tn/tn* mice. The frequency of γδT cells in the thymus showed no remarkable difference between wild-type and *tn/tn* mice during thymic ontogeny (Fig 7A). Absolute numbers of thymic γδT cells were reduced in *tn/tn* mice, because of the severe decrease in total thymic cellularity (Fig 1F).

It is known that the generation of murine γδT-cell subsets expressing distinct TCR-Vγ chains is developmentally regulated during ontogeny [30]. Vγ5$^+$ cells develop during the embryonic period, Vγ6$^+$ cells around birth, Vγ4$^+$ cells at the neonatal period, and Vγ1$^+$ cells at adult stages (according to the nomenclature of Heilig and Tonegawa [31]). These γδT-cell subsets distribute to different tissues in adult mice [30]: Vγ5$^+$ cells to epidermis, Vγ6$^+$ and Vγ4$^+$ cells to mucosal epithelia such as dermis, lung, tongue, and uterus, and Vγ1$^+$ cells to peripheral lymphoid organs. Although the proportion of Vγ5$^+$ and Vγ1$^+$ cells among thymic γδT cells was

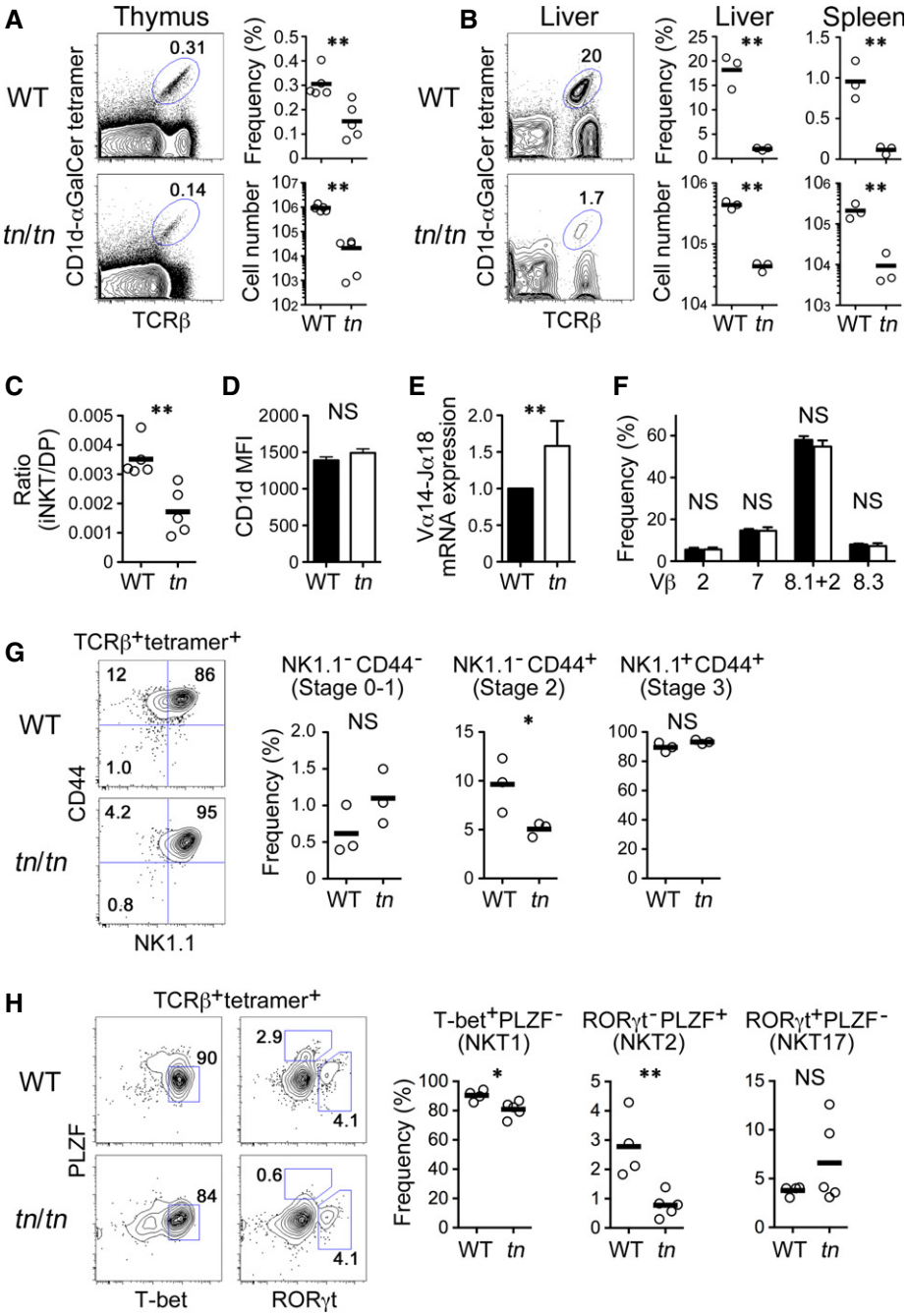

Figure 6. Reduced development of iNKT cells in *TN* mice.

A, B Thymocytes (A) or liver cells (B) from WT or *tn/tn* mice were stained with αGal-Cer/CD1d tetramer and anti-TCRβ antibody (left). The frequency and numbers of TCRβ$^+$ αGal-Cer/CD1d tetramer$^+$ cells from thymus (A), liver, or spleen (B) are shown (right) (n = 3–5).

C The ratio of TCRβ$^+$ tetramer$^+$ iNKT cells to DP thymocytes (n = 5).

D CD1d expression on DP thymocytes was equivalent between WT and *tn/tn* mice (n = 3–5).

E DP thymocytes were isolated from WT or *tn/tn* mice and analyzed by quantitative RT–PCR (n = 3). The level of Vα14-Jα18 transcript was normalized to TCR-Cα mRNA, and those in WT were arbitrarily set to 1.

F TCRβ$^+$ tetramer$^+$ thymic iNKT cells were further stained for Vβ2, Vβ7, Vβ8.1 + 2, or Vβ8.3 (n = 3–4).

G TCRβ$^+$ tetramer$^+$ thymic iNKT cells were further stained for NK1.1 and CD44. Representative flow cytometry profiles (left) and the frequency among total iNKT cells (right) of NK1.1$^-$CD44$^-$ (stage 0–1), NK1.1$^-$CD44$^+$ (stage 2), or NK1.1$^+$CD44$^+$ (stage 3) cells are shown (n = 3).

H TCRβ$^+$ tetramer$^+$ thymic iNKT cells were intracellularly stained for PLZF, T-bet, and RORγt. Representative flow cytometry profiles (left) and the frequency among total iNKT cells (right) of T-bet$^+$PLZF$^-$ (NKT1), RORγt$^-$PLZF$^+$ (NKT2), or RORγt$^+$PLZF$^-$ (NKT17) cells are shown (WT, n = 4; *tn/tn*, n = 5).

Data information: Data represent more than three independent experiments. Each circle represents an individual mouse, and horizontal bars indicate the mean (A, B, C, G, H). Mean ± SEM (D, E, F). The statistical significance was calculated with an unpaired one-tailed Student's t-test. *P < 0.05; **P < 0.01; NS, not significant.

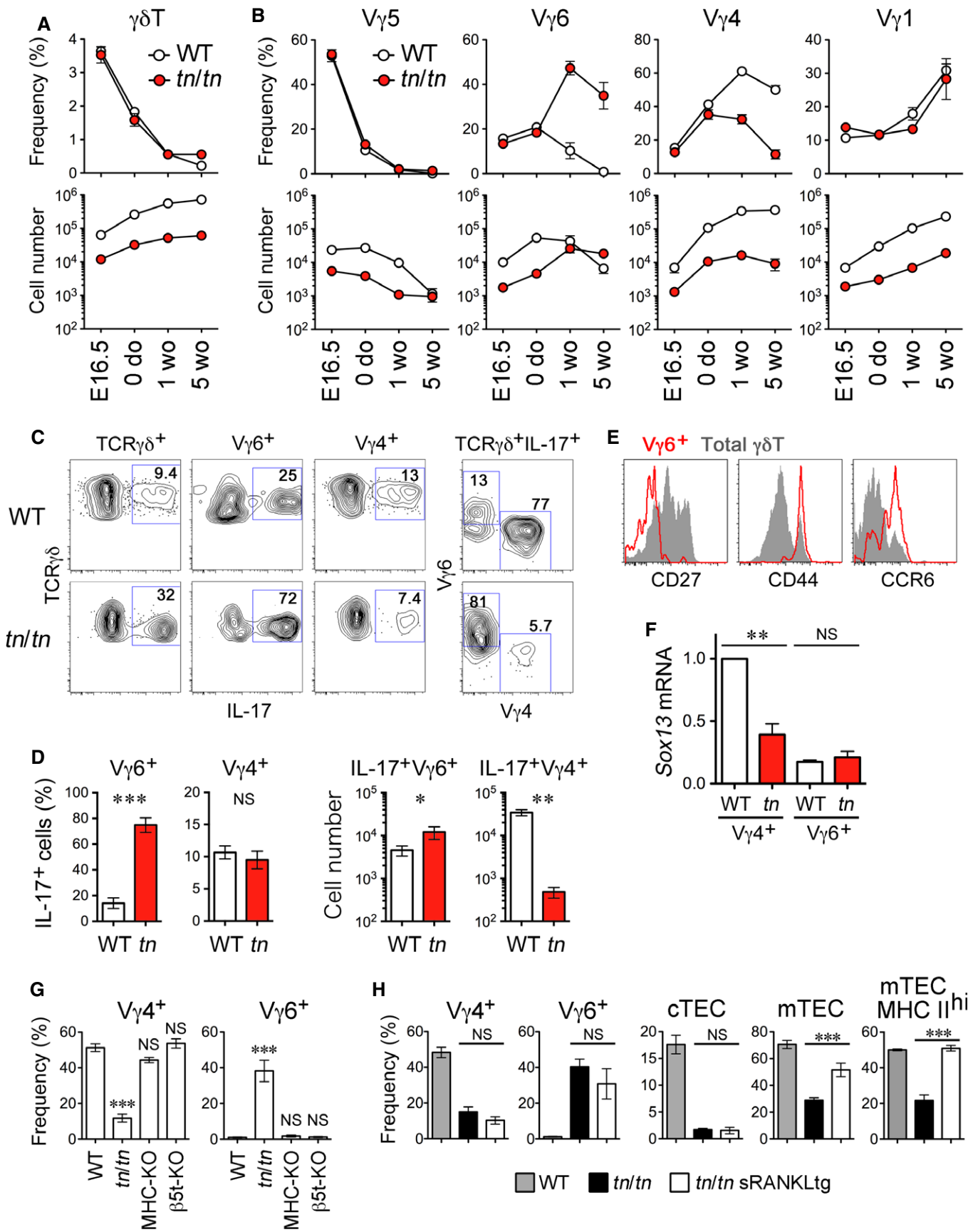

Figure 7.

Figure 7. Altered γδT17 TCR repertoire in *TN* mice.

A Frequency (% of total thymocytes) and numbers (per mouse) of thymic γδT cells from indicated ages of WT or *tn/tn* mice (n = 4–9).

B Frequency (% of total γδT cells) of Vγ5$^+$, Vγ6$^+$ (17D1$^+$ Vγ5$^-$), Vγ4$^+$, and Vγ1$^+$ cells and their numbers (per mouse) from indicated ages of WT or *tn/tn* mice (n = 3–8).

C Thymocytes from 5-week-old mice were cultured for 4 h with PMA, ionomycin, and brefeldin A and analyzed by flow cytometry.

D Frequency of IL-17-producing cells in Vγ6$^+$ or Vγ4$^+$ cells and absolute numbers of IL-17-producing Vγ6$^+$ and Vγ4$^+$ cells in individual mice (n = 4–5).

E Histograms show expression of CD27, CD44, and CCR6 in total γδT (shaded) and Vγ6$^+$ (red) cells from adult *tn/tn* mice.

F Quantitative RT–PCR analysis of *Sox13* in isolated Vγ4$^+$ or Vγ6$^+$ cells from WT or *tn/tn* mice (n = 4). *Sox13* mRNA expression was normalized to *Gapdh* mRNA, and those in WT Vγ4$^+$ cells were arbitrarily set to 1.

G Thymic γδT cells from 4- to 5-week-old WT, *tn/tn*, B6-*H-2Ab*$^{-/-}$*B2m*$^{-/-}$ (MHC-KO), or *Psmb11*$^{-/-}$ (β5t-KO) mice were analyzed for expression of Vγ4 and Vγ6 (n = 3–7).

H Frequency of Vγ4$^+$ or Vγ6$^+$ γδT cells (% of total thymic γδT cells), CD205^{hi}UEA1$^-$ cTECs or CD205^{lo}UEA1$^+$ mTECs (% of total TECs), and MHC class II^{hi} mTECs (% of total mTECs) from 4- to 7-week-old WT, *tn/tn*, or *tn/tn* sRANKL transgenic (tg) mice (n = 3–12).

Data information: Data represent more than two independent experiments. Graphs indicate mean ± SEM. The statistical significance between indicated groups was calculated with an unpaired one-tailed Student's t-test. *P < 0.05; **P < 0.01; ***P < 0.001; NS, not significant.

largely unchanged between wild-type and *tn/tn* mice throughout ontogeny (Fig 7B), development of Vγ6$^+$ and Vγ4$^+$ cells was dramatically altered in postnatal thymus from *tn/tn* mice. Vγ6$^+$ cells continued to expand after birth and their numbers exceeded those from wild-type thymus at 5 weeks old. In contrast, Vγ4$^+$ cells in *tn/tn* thymus did not show the robust postnatal increase that was apparent in wild-type thymus. TCR sequencing analysis demonstrated that Vγ6$^+$ cells expressed an invariant TCR-Vγ6-Jγ1 chain and Vγ4$^+$ γδT cells expressed a diverse TCR-Vγ4-Jγ1 repertoire, in both wild-type and *tn/tn* mice, representing qualitatively equivalent subpopulations (Supplementary Table S1).

Vγ6$^+$ and Vγ4$^+$ cells include an IL-17-producing subset, termed γδT17, whose development is restricted to the thymus during late embryonic and neonatal stages [32,33]; they also contribute to the pathogenesis of inflammation in the periphery [18–20]. In adult *tn/tn* mice, the proportion of IL-17-producing cells among γδT cells was greatly increased (Fig 5C). Among these γδT17 cells, the Vγ6$^+$ subset vigorously increased, whereas the Vγ4$^+$ subset substantially decreased, resulting in the marked skewing from Vγ4 to Vγ6 in TCR repertoire of γδT17 cells from *tn/tn* mice (Fig 7C and D). The majority of thymic Vγ6$^+$ cells in *tn/tn* mice were CD27$^-$ and expressed CD44 and CCR6, indicating that these are functionally mature cells (called γδ27$^-$) [34] (Fig 7E). Vγ4$^+$ cells from *tn/tn* mice exhibited reduced mRNA expression of Sox13 (Fig 7F), a key transcription factor for development of Vγ4$^+$ γδT17 cells [35,36]. These results indicate increased and prolonged production of functional Vγ6$^+$ γδT17 cells and restrained development of Vγ4$^+$ γδT17 cells in the thymus from *tn/tn* mice.

Proportions of Vγ4$^+$ and Vγ6$^+$ cells among thymic γδT cells was unaffected in both β5t-deficient mice and MHC-deficient mice that exhibit defective mTEC expansion (Fig 7G). Therefore, the altered repertoire of γδT cells was due to neither β5t deficiency nor reduced mTEC development. To further examine the effect of mTECs on γδT-cell repertoire, we utilized soluble RANKL (sRANKL) transgenic mice, causing enhanced expansion of mTECs [37]. Although introduction of sRANKL transgene rescued substantial number of MHC class II^{hi} mature mTECs in the thymus of *tn/tn* mice, altered repertoire of γδT cells was not rescued in mTEC-sufficient *tn/tn* sRANKL transgenic mice (Fig 7H and Supplementary Fig S5). These results clearly exclude the responsibility of β5t deficiency and reduced mTEC development to the altered repertoire of γδT cells observed in *tn/tn* thymus.

To explore the significance of the alteration in thymic γδT cells, we examined the distribution and function of peripheral γδT cells. In adult *tn/tn* mice, Vγ6$^+$ cells in lung were robustly increased, whereas Vγ4$^+$ cells were markedly reduced in lung, skin, spleen, and lymph nodes (Fig 8A). Lung Vγ6$^+$ γδT17 cells have been reported to trigger the inflammation induced by trehalose 6,6′-dimycolate (TDM), a cord factor of *Mycobacterium tuberculosis* [38]. Indeed, in response to TDM administration, *tn/tn* mice exhibited enhanced acute inflammatory responses in lung, including the production of IL-17 mRNA, organ swelling, and granuloma formation when compared with wild-type mice (Fig 8B–D), indicating that increased lung Vγ6$^+$ γδT17 cells are functionally normal. To the contrary, in the skin, psoriasis-like dermatitis induced by imiquimod (IMQ), in which Vγ4$^+$ γδT17 cells that expand in lymph node and home to inflamed skin play a crucial role [35,39,40], was significantly attenuated in *tn/tn* mice (Fig 8E and F). These results indicate that the γδT cells generated in the absence of mature cTECs express an altered TCR repertoire that fails to properly mount inflammatory responses.

Discussion

In the current study, we established a novel mouse model, designated *TN* mice, which intrinsically lacks mature cTECs. We identified the G220R mutation of β5t as being primarily responsible for cTEC deficiency in *TN* mice. Thus, *TN* is a β5t-driven, mature cTEC-deficient mouse strain, which will be useful to investigate the physiological significance of cTECs.

It is interesting to note that in the thymus from *tn/tn* mice, the compartmentalization of cortex and medulla is readily detectable, despite the loss of mature cTECs. It was reported that outward migration of developing thymocytes from the corticomedullary junction to the cortex requires CXCL12-CXCR4 and CCL25-CCR9 chemokine signals [41,42]. However, the expression of CXCL12 and CCL25 in CD205^{lo}UEA1$^-$ TECs from *tn/tn* mice is very low, ~6 and 0.3%, respectively, compared with that in wild-type mature cTECs. Another thymic chemokine CCL21, which attracts mature CD4SP and CD8SP thymocytes from the cortex to the medulla [5], is normally produced by mTECs in *tn/tn* mice. These results demonstrate that the cortex/medulla compartmentalization in the thymus does not require mature cTECs and can be mediated by CD205^{lo}UEA1$^-$ immature TECs along with CCL21-expressing mTECs. Further studies will be needed to dissect developmental processes of cTECs and to better understand their nature and function.

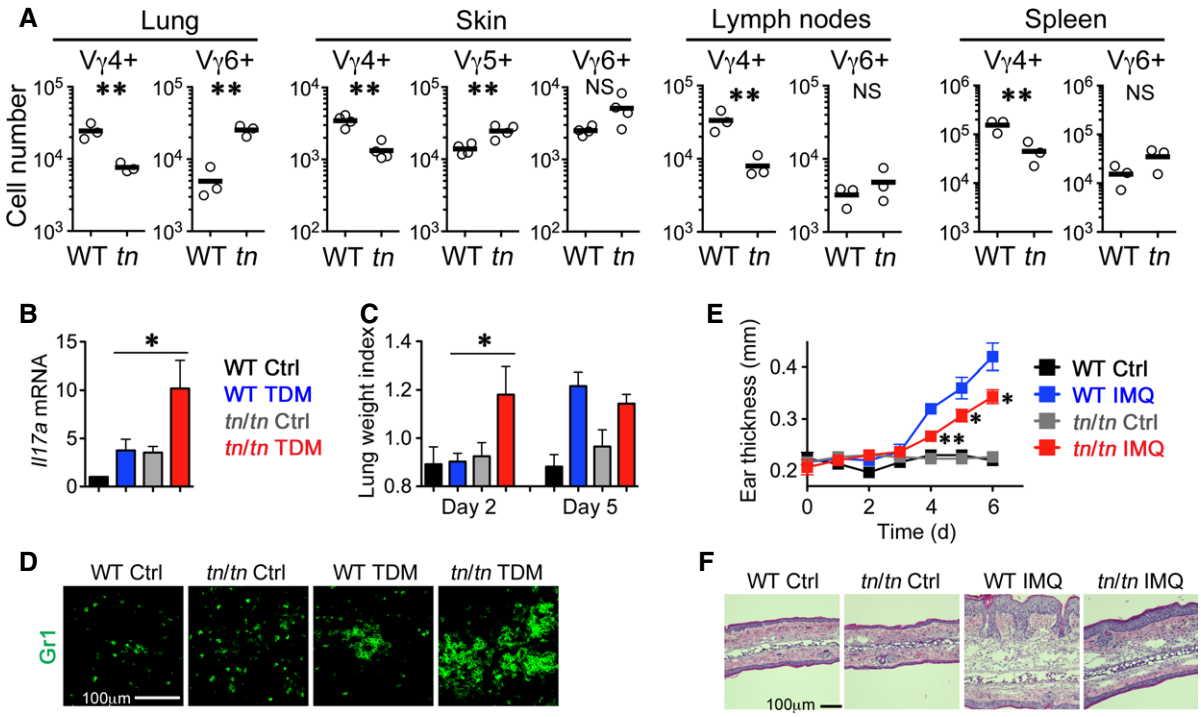

Figure 8. *TN* mice exhibited altered γδT-cell-mediated inflammatory responses.

A Absolute numbers (per mouse) of indicated γδT-cell subsets in lung, skin, lymph nodes (inguinal, axillary, and submandibular), and spleen from 5-week-old WT or *tn/tn* mice ($n = 3$). Each circle represents an individual mouse, and horizontal bars indicate the mean. The statistical significance was calculated with an unpaired one-tailed Student's *t*-test. $^*P < 0.05$; $^{**}P < 0.01$; NS, not significant.

B–D WT or *tn/tn* mice were injected intravenously with an oil-in-water emulsion containing TDM (15 μg). Emulsion without TDM was injected as a vehicle control. *Il17a* mRNA levels in lungs at day 2 were examined by quantitative RT–PCR and normalized to *Gapdh* mRNA ($n = 3$–4, mean ± SEM) (B). Lung inflammation intensity was measured by calculating the lung weight index ($n = 3$–5, mean ± SEM) (C). The statistical significance between TDM-treated WT and *tn/tn* mice was calculated with an unpaired one-tailed Student's *t*-test. $^*P < 0.05$. Lung sections at day 2 were stained for granulocyte marker Gr1 (D).

E, F WT or *tn/tn* mice were treated daily for 6 days with IMQ cream or control cream on the ears. Ear skin thickness at the days indicated ($n = 3$, mean ± SEM) (E). The statistical significance between IMQ-treated WT and *tn/tn* mice was calculated with an unpaired one-tailed Student's *t*-test. $^*P < 0.05$; $^{**}P < 0.01$. HE staining of the ear section at day 6 (F).

Although the thymic cortex is apparently formed, cortical T-cell development without mature cTECs is obviously abnormal, as *tn/tn* mice showed impairment of positive selection of αβT cells. *tn/tn* mouse thymi showed diminished expression of cathepsin L, Prss16 (also called thymus-specific serine protease), and complete loss of β5t-containing thymoproteasomes. Cathepsin L and Prss16 are endosomal/lysosomal proteases highly expressed by cTECs that regulate positive selection of MHC class II-restricted CD4 T cells [12,13]. Thymoproteasomes are essential for positive selection of MHC class I-restricted CD8 T cells, likely by producing cTEC-specific MHC class I-bound peptides [8,10,11]. Our results that *tn/tn* mice have an altered TCR-Vα and TCR-Vβ distribution of both CD4 and CD8 T cells indicate that cTECs contribute not only to generate the optimum cellularity of T cells but also to shape their αβTCR repertoire, as suggested by previous reports. In addition to the lack of such functional molecules in the cortex, it is also possible that a loss of the cortical epithelial network *per se* impairs thymocyte development through physical interference with intracortical migration or cell–cell interactions of cortical thymocytes. Taken together, cortex-resident, immature TECs in *tn/tn* thymus are incompetent for αβT-cell repertoire formation, even though they are functional in forming the thymic cortex and supporting development of a small fraction of αβT cells, confirming the essential role for cTECs in development and repertoire formation of conventional αβT cells.

To the contrary, negative selection of *mtv* superantigen-reactive thymocytes occurred normally in *tn/tn* mice. Indeed, no signs of systemic autoimmunity were detected in *tn/tn* mice (unpublished observation), indicating that self-tolerance is established in the absence of mature cTECs. Although a recent report indicated that three quarters of negative selection occurs in the cortex [43], negative selection was not affected in the absence of mature cTECs. Therefore, cortex-resident, immature TECs and/or dendritic cells [44] may induce negative selection of self-reactive thymocytes.

The most unexpected finding from the current study was the influence of mature cTEC deficiency on γδT-cell development. γδT cells generated in the absence of mature cTECs were skewed toward IL-17-producing (γδT17) lineage that expressed an altered γδTCR repertoire. As the development of $V\gamma5^+$ and $V\gamma1^+$ γδT cells (mostly non-γδT17 cells) was normal in *tn/tn* thymus, the influence of mature cTEC deficiency is specific to γδT17 lineage. It was shown that development of γδT cells in the thymus is dependent on IL-7 [45], and expansion and development of γδT17 cells requires IL-7 [46] and Dll4-Notch signals [47], respectively. As *tn/tn* mice lack mature cTECs that express high levels of IL-7 and Dll4, the increase

of γδT17 cells seen in the *tn/tn* thymus could not be directly attributed to signaling on these molecules. It may be that relatively low levels of expression of IL-7 and Dll4 by immature TECs and mTECs, and also likely by other thymic stromal cells, are sufficient for inducing development of γδT17 cells. Most interestingly, two major subsets of γδT17 cells, $V\gamma6^+$ cells and $V\gamma4^+$ cells, are reciprocally differentiated in *tn/tn* mice. Increased and prolonged production of $V\gamma6^+$ cells resulted in boosted $V\gamma6^+$ γδT17-mediated inflammatory responses, and impaired production of $V\gamma4^+$ cells, which in turn provided protection from $V\gamma4^+$ γδT17-dependent dermatitis. The altered repertoire of γδT cells in *tn/tn* mice was due to neither β5t deficiency nor reduced mTEC development, as the distribution of $V\gamma4^+$ and $V\gamma6^+$ cells was unaffected in β5t-deficient mice and mTEC-reduced, MHC-deficient mice, and the altered γδT-cell repertoire in *tn/tn* mice was not restored by sRANKL-mediated enhancement of mTEC differentiation. These results suggest that mature cTECs play roles in repressing the development of $V\gamma6^+$ cells and promoting that of $V\gamma4^+$ cells, although it is also possible that cortex-resident, immature TECs in *tn/tn* mice have reciprocal functions and that partly defective development of (likely RANKL-independent) mTECs in *tn/tn* mice caused the γδT17 repertoire alteration. A recent study showed a differential developmental requirement for $V\gamma4^+$ and $V\gamma6^+$ γδT17 cells; $V\gamma6^+$ γδT17 cells absolutely require fetal thymus for their development, whereas $V\gamma4^+$ γδT17 cells can be generated in adult thymus [48]. Thus, it is suggested that the thymus from adult *tn/tn* mice provides fetal type microenvironment that supports predominant development of $V\gamma6^+$ γδT17 cells.

Our results first reveal that cTECs determine the balance between $V\gamma4^+$ and $V\gamma6^+$ γδT-cell development, which is important for properly mounting inflammatory responses. The mechanisms by which cTECs regulate the γδT17 TCR repertoire remain to be elucidated. Mature cTECs and immature TECs may express different cell-surface proteins, such as Skint family proteins [49], or as of yet unidentified selecting ligand molecule(s), that mediate differentiation or deletion of $V\gamma4^+$ or $V\gamma6^+$ γδT cells; for example, as mTECs support maturation of $V\gamma5^+$ cells via expression of Skint1 [17,50]. The conversion of the Vγ repertoire in *tn/tn* mice could be attributed to the alternation of interaction between the γδTCRs and its putative ligands on TECs, because recent studies proposed that strength of ligand–γδTCR interaction controls lineage commitment and specification of effector fate of γδT cells [16,20,51]. It is also possible that restricted access of developing γδT cells to cTECs [52] or reduced negative feedback of γδT17 development by αβT cells [33] may be responsible for the repertoire conversion in *tn/tn* mice. We observed reduced expression of the transcription factor Sox13 in $V\gamma4^+$ γδT cells from cTEC-deficient *tn/tn* mice. Interestingly, deficiency of Sox13 in mice resulted in the loss of $V\gamma4^+$ γδT17 cell development but a partial reduction of $V\gamma4^-$ (likely to be $V\gamma6^+$) γδT17 cells [35,36]. Therefore, the conversion of the γδT17 repertoire in *tn/tn* mice could be partly explained by the decrease of Sox13, caused by the absence of proper interaction with cTECs.

Taken together, the present study, utilizing a newly established mouse strain that lacks mature cTECs, provides novel evidence for γδT-cell repertoire determination by thymic epithelium. cTECs are required for the shaping of the TCR repertoire, not only of conventional αβT-cell subsets, but also of an "innate-type" γδT-cell subset programmed for IL-17 production. Future studies to clarify the molecular mechanisms should unveil developmental rules for γδT cells that can be applied to γδT-cell-based immunotherapies.

Materials and Methods

Mice

C57BL/6, BALB/c, and C57BL/6× DBA/2F1 (BDF1) mice were purchased from SLC Japan (Shizuoka, Japan). *TN* mice were derived from an in-house breeding colony of a C57BL/6NCrSlc strain originally derived from SLC Japan. B6.SJL-*Ptprca* (B6-CD45.1) mice were purchased from Taconic Farm (NY, USA). *Psmb11*$^{-/-}$ mice [8], OT-I TCR transgenic mice [53], OT-II TCR transgenic mice [54], *Rag2*$^{-/-}$ mice [55], *H-2Ab*$^{-/-}$ mice [56], *B2m*$^{-/-}$ mice [57], and sRANKL transgenic mice [58] were described previously. All mice were bred and maintained under specific pathogen-free conditions in our animal facility. All animal experiments were approved by the Animal Care and Use Committee of the National Center for Global Health Medicine (NCGM) Research Institute (number: 23-Tg-31) and conducted in accordance with institutional procedures.

Flow cytometry and cell sorting

Flow cytometry analysis and cell sorting were performed with FACSCantoII and FACSAriaIII (BD Bioscience) as previously described [59]. Thymic stromal cells were prepared by digesting thymic fragments with collagenase D (Roche) and DNase I (Roche), as described [60]. For intracellular staining, cells were fixed with 2% paraformaldehyde for 30 min, permeabilized with 0.1% saponin, and stained with antibodies. Foxp3 staining was performed using the Foxp3 staining kit (eBioscience) according to the manufacturer's protocol.

Antibodies

Monoclonal antibodies specific for B220 (RA3-6B2), CD4 (GK1.5), CD5 (53-7.3), CD8α (53-6.7), CD8β (CT-CD8b), CD25 (PC61.5), CD69 (H1.2F3), CD205 (205yekta), NK1.1 (PK136), TCRβ (H57-597), Vα11 (RR8-1), Aire (5H12), PLZF (Mags.21F7), and RORγt (B2D) were purchased from eBioscience. Monoclonal antibodies against CD3ε (2C11), CD44 (IM7), CD45 (30-F11), CD45.1 (A20), CD45.2 (104), EpCAM (G8.8), Ly51 (6C3), CCR6 (29-2L17), TCRγδ (GL3), TCR-Vγ1 (2.11), TCR-Vγ4 (UC3-10A6), TCR-Vγ5 (536), IL-17 (TC11-18H10.1), and T-bet (4B10) were purchased from BioLegend. Mouse Vβ TCR screening panel and anti-Vα2 (B20.1) monoclonal antibody were purchased from BD PharMingen. Anti-pan-keratin (C-11) and anti-FLAG (M2) monoclonal antibodies were purchased from Sigma-Aldrich. UEA1 was purchased from Vector Laboratories. Polyclonal antibodies for keratin 5 (Covance), keratin 8 (Progen), keratin 14 (Covance), and CCL21 (R&D Systems) were used. Monoclonal antibody 17D1 specific for TCR-Vγ6/Vδ1 and TCR-Vγ5/Vδ1 was provided by Dr. Robert E. Tigelaar (Yale University) and used as described previously [61]. Polyclonal antibody for β5t was described previously [8]. Anti-polyubiquitin monoclonal antibody (FK2) was purchased from MBL.

Bone marrow chimera

Bone marrow cells obtained from donor mice were depleted of T cells using biotin-conjugated anti-CD4, anti-CD8, and anti-Thy1.2 antibodies and streptavidin-conjugated magnetic beads (Miltenyi Biotec). Recipient mice were X-ray-irradiated (9.25 Gy) and injected with T-cell-depleted bone marrow cells (4×10^7 cells) 1 day after irradiation. Mice were analyzed 5 weeks after the injection.

Histological analysis

Frozen tissues embedded in OCT compound (Sakura Finetek) were sliced into 5-μm-thick sections by cryostat (Leica), air-dried, fixed with acetone, and stained with hematoxylin and eosin, or with specific antibodies as described previously [21]. Multi-color images were obtained by BZ-9000 fluorescent microscope (Keyence).

Electron microscopy

Thymus lobes from 5-week-old mice were fixed and analyzed by scanning electron microscopy at Tokai Electron Microscopy Analysis (Aichi, Japan).

Fetal thymic organ culture

Thymic lobes isolated from E14.5 fetuses were cultured as previously described [62]. To induce mTEC development, recombinant soluble RANKL (1 μg/ml) (Wako) was added to the medium.

Quantitative mRNA analysis

Total cellular RNA was reverse-transcribed with Superscript III first-strand synthesis supermix for qRT–PCR (Life Technologies). Real-time PCR was performed with SYBR Premix ExTaq (TaKaRa) and StepOne real-time PCR system (Life Technologies). Primer sequences are available upon request.

Identification of the responsible mutation of *TN* mice

For linkage analysis, *TN* mice originated from C57BL/6 background were crossed with BALB/c mice. Seventy-seven mice (55%) out of 139 (*TN* × BALB/c) N2 mice exhibited thymic hypoplasia and naïve T lymphopenia, which confirmed that the trait of this mutation was dominant. Genomic DNA was prepared from tail biopsies by the standard method of SDS/proteinase K lysis followed by phenol/chloroform. Information on microsatellite markers was obtained from Mouse Genome Informatics (MGI; http://www.informatics.jax.org/). For sequencing the candidate region, the SureSelect Target Enrichment System (Agilent Technologies) was used to enrich for 11.2-Mb genomic region between D14Mit121 and D14Mit113. Enriched DNA fragments were sequenced by HiSeq 2000 (Illumina).

CRISPR/Cas9-mediated genome editing in mice

Single-guide (sg) RNA was designed for the target sequence (5′-TGCTTATTCAAGGGGCTCAGTGG-3′) and prepared as described previously [63] with some modifications. Briefly, sgRNA expression vector for target sequence with a T7 promoter was synthesized (Operon Biotechnologies, Tokyo, Japan), and transcribed *in vitro* using MEGAshortscript kit (Life Technologies). *hCas9* sequence was removed from pX330 (http://www.addgene.org/42330) and placed under the T7 promoter. *hCas9* mRNA was synthesized using mMESSAGE mMACHINE T7 kit (Life Technologies) and was polyadenylated with polyA tailing kit (Life Technologies). The sgRNAs and *hCas9* mRNAs were purified by phenol/chloroform/isoamylalchol extraction and concentrated by ethanol precipitation. For injection into one-cell embryos, fertilized eggs were obtained by *in vitro* fertilization as described previously [64]. *hCas9* mRNAs (100 ng/μl) and sgRNAs (50 ng/μl) were co-injected into the cytoplasm of the pronuclear stage eggs. For generating targeted mutant mice, WT oligonucleotide (5′-GAAGCCTACACCCTGGCCCGCTGTGCTGTGGCCCATGCCACCCACCGTGATGCTTATTCAGGGGGCTCAGTGGACCTCTTCCACGTTCGGGAGAGCGGATGGGAGTATGTATCCCGCAGT-3′) (100 ng/μl) was co-injected. The eggs were transferred into the oviducts of pseudopregnant ICR female mice. The efficiency of targeted gene disruption and potential off-target effects are shown in Supplementary Tables S2 and S3.

Cell culture and retrovirus infection

Mouse embryonic fibroblasts isolated from *Psmb8*$^{-/-}$ (β5i$^{-/-}$) mice [65], Swiss 3T3 cells (ATCC), and ST2 cells (kindly provided by Dr. Meinrad Busslinger) were cultured in DMEM medium supplemented with 10% fetal calf serum (FCS), penicillin, and streptomycin (Life Technologies). DNA fragments encoding an open-reading frame of mouse β5t^{WT} or β5t^{G220R} were cloned into the retrovirus vector pMRX-IRES-EGFP [66]. Retrovirus supernatant was prepared as described previously [62].

Proteasomal analysis

Glycerol density gradient was described previously [67]. For immunoprecipitation, cells were lysed in an ice-cold lysis buffer (50 mM Tris–HCl (pH 7.5), 150 mM NaCl, 5 mM $MgCl_2$, 0.5% NP-40, and protease inhibitor cocktail (Thermo)). Cell lysates were incubated with agarose-bead-conjugated anti-FLAG M2 antibody or anti-β5t antibody followed by sepharose bead-conjugated protein G (GE Healthcare). The beads were then washed and boiled in Laemmli gel-loading buffer. The proteins were separated by SDS–PAGE [15% Bis-Tris gel (Life Technologies)] or native PAGE [7% Tris-acetate gel (Life Technologies)], transferred onto PVDF membrane, and detected with indicated antibodies.

Preparation of tissue-resident lymphocytes

IELs were prepared as described elsewhere with some modifications [59]. Briefly, small intestine was isolated and Peyer's patches were completely removed prior to opening longitudinally. After six quick rinses in PBS, the intestine was cut into 5-mm pieces, followed by incubating twice in calcium/magnesium-free HBSS containing 2% FCS and 2 mM EDTA at 37°C for 20 min. The cell suspension was filtered through glass wool and the filtrate was centrifuged in 30% Percoll (GE Healthcare) to remove mucus. Cell pellets were then resuspended with 40% Percoll and further separated through a 40–70% Percoll step gradient. The cells at the interface of the Percoll

gradient were collected and used for further analysis. For isolation of lymphocytes from skin or lung, ears or lungs from adult mice were cut into small pieces and digested with 0.2% collagenase D (Roche) and DNase I (Roche) at 37°C for 30 min. After digestion, tissue fragments were mechanically disrupted using a syringe and 18-G needle, and cells were passed through 100-μm nylon mesh to remove tissue clumps, collected by centrifugation, and resuspended in PBS containing 2 mM EDTA and 2% FCS.

Inflammatory responses

Adult mice (6 to 12 week old) were injected intravenously with 100 μl of emulsion containing 15 μg TDM (Sigma) prepared as described previously [68]. Lung weight index was calculated as described previously [69]. Emulsion without TDM was injected as a control. For testing psoriasis-like dermatitis, a daily dose of 5 mg of Beselna cream (5% imiquimod; Mochida Pharmaceutical) or control vaseline cream (Wako) was applied to each ear for 6 days. At the days indicated, the ear thickness was measured using a micrometer.

Sequencing analysis of TCRγ

$V\gamma4^+$ or $V\gamma6^+$ ($17D1^+$ $V\gamma5^-$) thymic γδT cells were isolated from 3- to 4-week-old wild-type or *tn/tn* mice (pooled from three mice per group). Total cellular RNA was extracted using RNeasy micro kit (QIAGEN) and reverse-transcribed with oligo-dT primer and Superscript III reverse transcriptase (Life Technologies). Vγ4-Cγ1 and Vγ6-Cγ1 cDNA fragments were PCR-amplified and cloned in the pBluescript vector. DNA sequences of randomly picked clones were determined. Primer sequences are as follows: Vγ4 forward, 5-C TTGCAACCCCTACCCATAT-3′; Vγ6 forward, 5-TCAAGAGGAAAGG AAATACGGC-3′; and Cγ1 reverse, 5-CTGGGAGTCCAGGATAGTA TTG-3′.

Statistical analysis

The statistical significance was calculated with an unpaired one-tailed Student's *t*-test. When indicated, one-way ANOVA was used. All calculations and justifications were done using the GraphPad Prism software. No randomization or exclusion of samples was used. For animal experiments, sample size was chosen based on previous experience and preliminary experiments. No blinding of investigators was done.

Supplementary information for this article is available online: http://embor.embopress.org

Acknowledgements

We thank Dr. Robert E. Tigelaar for providing 17D1 antibody; Drs. Kensuke Shibata and Yasunobu Yoshikai for helpful discussion; and Dr. Michael S. Patrick for reading the manuscript. This study was supported by Grants-in-Aid for Research from the Ministry of Education, Culture, Sports, and Technology in Japan (25111516), the grant for National Center for Global Health and Medicine (24-112), Astellas Foundation, Inamori Foundation, and Kanae Foundation.

Author contributions

TNi and HS designed the project. TNi, RM, SN, HO, TNa, and HT performed experiments on mouse, tissue, and cell analysis. YS, MG, RY, and TO worked on the linkage analysis and CRISPR/Cas9-mediated genome editing; YO and SM worked on the proteasome analysis. HY analyzed sRANKLtg mice. TNit and HS wrote the manuscript with help from the other authors.

Conflict of interest

The authors declare that they have no conflict of interest.

References

1. Anderson G, Takahama Y (2012) Thymic epithelial cells: working class heroes for T cell development and repertoire selection. *Trends Immunol* 33: 256 – 263
2. Klein L, Kyewski B, Allen PM, Hogquist KA (2014) Positive and negative selection of the T cell repertoire: what thymocytes see (and don't see). *Nat Rev Immunol* 14: 377 – 391
3. Akiyama T, Shinzawa M, Qin J, Akiyama N (2013) Regulations of gene expression in medullary thymic epithelial cells required for preventing the onset of autoimmune diseases. *Front Immunol* 4: 249 – 249
4. Tykocinski L-O, Sinemus A, Kyewski B (2008) The thymus medulla slowly yields its secrets. *Ann NY Acad Sci* 1143: 105 – 122
5. Ueno T, Saito F, Gray DHD, Kuse S, Hieshima K, Nakano H, Kakiuchi T, Lipp M, Boyd RL, Takahama Y (2004) CCR7 signals are essential for cortex-medulla migration of developing thymocytes. *J Exp Med* 200: 493 – 505
6. Cowan JE, Parnell SM, Nakamura K, Caamano JH, Lane PJL, Jenkinson EJ, Jenkinson WE, Anderson G (2013) The thymic medulla is required for Foxp3(+) regulatory but not conventional CD4(+) thymocyte development. *J Exp Med* 210: 675 – 681
7. White AJ, Jenkinson WE, Cowan JE, Parnell SM, Bacon A, Jones ND, Jenkinson EJ, Anderson G (2014) An essential role for medullary thymic epithelial cells during the intrathymic development of invariant NKT cells. *J Immunol* 192: 2659 – 2666
8. Murata S, Sasaki K, Kishimoto T, Niwa S-I, Hayashi H, Takahama Y, Tanaka K (2007) Regulation of $CD8^+$ T cell development by thymus-specific proteasomes. *Science* 316: 1349 – 1353
9. Ripen AM, Nitta T, Murata S, Tanaka K, Takahama Y (2011) Ontogeny of thymic cortical epithelial cells expressing the thymoproteasome subunit β5t. *Eur J Immunol* 41: 1278 – 1287
10. Nitta T, Murata S, Sasaki K, Fujii H, Ripen AM, Ishimaru N, Koyasu S, Tanaka K, Takahama Y (2010) Thymoproteasome shapes immunocompetent repertoire of CD8(+) T cells. *Immunity* 32: 29 – 40
11. Xing Y, Jameson SC, Hogquist KA (2013) Thymoproteasome subunit-β5T generates peptide-MHC complexes specialized for positive selection. *Proc Natl Acad Sci USA* 110: 6979 – 6984
12. Honey K, Nakagawa T, Peters C, Rudensky A (2002) Cathepsin L regulates CD4(+) T cell selection independently of its effect on invariant chain: a role in the generation of positively selecting peptide ligands. *J Exp Med* 195: 1349 – 1358
13. Gommeaux J, Gregoire C, Nguessan P, Richelme M, Malissen M, Guerder S, Malissen B, Carrier A (2009) Thymus-specific serine protease regulates positive selection of a subset of CD4(+) thymocytes. *Eur J Immunol* 39: 956 – 964
14. Assarsson E, Chambers BJ, Hogstrand K, Berntman E, Lundmark C, Fedorova L, Imreh S, Grandien A, Cardell S, Rozell B *et al* (2007) Severe defect in thymic development in an insertional mutant mouse model. *J Immunol* 178: 5018 – 5027

15. Rode I, Boehm T (2012) Regenerative capacity of adult cortical thymic epithelial cells. *Proc Natl Acad Sci USA* 109: 3463 – 3468
16. Prinz I, Silva-Santos B, Pennington DJ (2013) Functional development of γδT cells. *Eur J Immunol* 43: 1988 – 1994
17. Roberts NA, White AJ, Jenkinson WE, Turchinovich G, Nakamura K, Withers DR, McConnell FM, Desanti GE, Benezech C, Parnell SM *et al* (2012) Rank signaling links the development of invariant γδT cell progenitors and Aire(+) medullary epithelium. *Immunity* 36: 427 – 437
18. Becher B, Pantelyushin S (2012) Hiding under the skin Interleukin-17-producing γδT cells go under the skin? *Nat Med* 18: 1748 – 1750
19. Chien Y-h, Zeng X, Prinz I (2013) The natural and the inducible interleukin (IL)-17-producing γδT cells. *Trends Immunol* 34: 151 – 154
20. Vantourout P, Hayday A (2013) Six-of-the-best: unique contributions of γδT cells to immunology. *Nat Rev Immunol* 13: 88 – 100
21. Hikosaka Y, Nitta T, Ohigashi I, Yano K, Ishimaru N, Hayashi Y, Matsumoto M, Matsuo K, Penninger JM, Takayanagi H *et al* (2008) The cytokine RANKL produced by positively selected thymocytes Fosters medullary thymic epithelial cells that express autoimmune regulator. *Immunity* 29: 438 – 450
22. Shakib S, Desanti GE, Jenkinson WE, Parnell SM, Jenkinson EJ, Anderson G (2009) Checkpoints in the development of thymic cortical epithelial cells. *J Immunol* 182: 130 – 137
23. Ohigashi I, Zuklys S, Sakata M, Mayer CE, Zhanybekova S, Murata S, Tanaka K, Hollaender GA, Takahama Y (2013) Aire-expressing thymic medullary epithelial cells originate from β5t-expressing progenitor cells. *Proc Natl Acad Sci USA* 110: 9885 – 9890
24. Baik S, Jenkinson EJ, Lane PJL, Anderson G, Jenkinson WE (2013) Generation of both cortical and Aire$^+$ medullary thymic epithelial compartments from CD205$^+$ progenitors. *Eur J Immunol* 43: 589 – 594
25. Alves NL, Takahama Y, Ohigashi I, Ribeiro AR, Baik S, Anderson G, Jenkinson WE (2014) Serial progression of cortical and medullary thymic epithelial microenvironments. *Eur J Immunol* 44: 16 – 22
26. Nandi D, Tahiliani P, Kumar A, Chandu D (2006) The ubiquitin-proteasome system. *J Biosci* 31: 137 – 155
27. Seifert U, Bialy LP, Ebstein F, Bech-Otschir D, Voigt A, Schroeter F, Prozorovski T, Lange N, Steffen J, Rieger M *et al* (2010) Immunoproteasomes preserve protein homeostasis upon interferon-induced oxidative stress. *Cell* 142: 613 – 624
28. Gapin L, Matsuda JL, Surh CD, Kronenberg M (2001) NKT cells derive from double-positive thymocytes that are positively selected by CD1d. *Nat Immunol* 2: 971 – 978
29. Lee YJ, Holzapfel KL, Zhu J, Jameson SC, Hogquist KA (2013) Steady-state production of IL-4 modulates immunity in mouse strains and is determined by lineage diversity of iNKT cells. *Nat Immunol* 14: 1146 – 1154
30. Carding SR, Egan PJ (2002) γδT cells: functional plasticity and heterogeneity. *Nat Rev Immunol* 2: 336 – 345
31. Heilig JS, Tonegawa S (1986) Diversity of murine gamma genes and expression in fetal and adult lymphocytes-T. *Nature* 322: 836 – 840
32. Shibata K, Yamada H, Nakamura R, Sun X, Itsumi M, Yoshikai Y (2008) Identification of CD25$^+$ γδT cells as fetal thymus-derived naturally occurring IL-17 producers. *J Immunol* 181: 5940 – 5947
33. Haas JD, Ravens S, Dueber S, Sandrock I, Oberdoerfer L, Kashani E, Chennupati V, Foehse L, Naumann R, Weiss S *et al* (2012) Development of interleukin-17-producing γδT cells is restricted to a functional embryonic wave. *Immunity* 37: 48 – 59
34. Ribot JC, deBarros A, Pang DJ, Neves JF, Peperzak V, Roberts SJ, Girardi M, Borst J, Hayday AC, Pennington DJ *et al* (2009) CD27 is a thymic determinant of the balance between Interferon-γ-and Interleukin 17-producing γδT cell subsets. *Nat Immunol* 10: 427 – 436
35. Gray EE, Ramirez-Valle F, Xu Y, Wu S, Wu Z, Karjalainen KE, Cyster JG (2013) Deficiency in IL-17-committed Vγ4(+) γδT cells in a spontaneous Sox13-mutant CD45.1(+) congenic mouse substrain provides protection from dermatitis. *Nat Immunol* 14: 584 – 592
36. Malhotra N, Narayan K, Cho OH, Sylvia KE, Yin C, Melichar H, Rashighi M, Lefebvre V, Harris JE, Berg LJ *et al* (2013) A network of high-mobility group box transcription factors programs innate interleukin-17 production. *Immunity* 38: 681 – 693
37. Ohigashi I, Nitta T, Lkhagvasuren E, Yasuda H, Takahama Y (2011) Effects of RANKL on the thymic medulla. *Eur J Immunol* 41: 1822 – 1827
38. Saitoh T, Yano I, Kumazawa Y, Takimoto H (2012) Pulmonary TCR gamma delta T cells induce the early inflammation of granuloma formation by a glycolipid trehalose 6,6′-dimycolate (TDM) isolated from *Mycobacterium tuberculosis*. *Immunopharmacol Immunotoxicol* 34: 815 – 823
39. Cai Y, Shen X, Ding C, Qi C, Li K, Li X, Jala VR, Zhang H-G, Wang T, Zheng J *et al* (2011) Pivotal role of dermal IL-17-producing γδT cells in skin inflammation. *Immunity* 35: 649 – 649
40. Pantelyushin S, Haak S, Ingold B, Kulig P, Heppner FL, Navarini AA, Becher B (2012) Ror γt(+) innate lymphocytes and γδT cells initiate psoriasiform plaque formation in mice. *J Clin Invest* 122: 2252 – 2256
41. Plotkin J, Prockop SE, Lepique A, Petrie HT (2003) Critical role for CXCR4 signaling in progenitor localization and T cell differentiation in the postnatal thymus. *J Immunol* 171: 4521 – 4527
42. Benz C, Heinzel K, Bleul CC (2004) Homing of immature thymocytes to the subcapsular microenvironment within the thymus is not an absolute requirement for T cell development. *Eur J Immunol* 34: 3652 – 3663
43. Stritesky GL, Xing Y, Erickson JR, Kalekar LA, Wang X, Mueller DL, Jameson SC, Hogquist KA (2013) Murine thymic selection quantified using a unique method to capture deleted T cells. *Proc Natl Acad Sci USA* 110: 4679 – 4684
44. McCaughtry TM, Baldwin TA, Wilken MS, Hogquist KA (2008) Clonal deletion of thymocytes can occur in the cortex with no involvement of the medulla. *J Exp Med* 205: 2575 – 2584
45. Shitara S, Hara T, Liang B, Wagatsuma K, Zuklys S, Hollaender GA, Nakase H, Chiba T, Tani-ichi S, Ikuta K (2013) IL-7 produced by thymic epithelial cells plays a major role in the development of thymocytes and TCRγδ(+) intraepithelial lymphocytes. *J Immunol* 190: 6173 – 6179
46. Michel M-L, Pang DJ, Haque SFY, Potocnik AJ, Pennington DJ, Hayday AC (2012) Interleukin 7 (IL-7) selectively promotes mouse and human IL-17-producing γδ cells. *Proc Natl Acad Sci USA* 109: 17549 – 17554
47. Shibata K, Yamada H, Sato T, Dejima T, Nakamura M, Ikawa T, Hara H, Yamasaki S, Kageyama R, Iwakura Y *et al* (2011) Notch-Hes1 pathway is required for the development of IL-17-producing γδT cells. *Blood* 118: 586 – 593
48. Cai Y, Xue F, Fleming C, Yang J, Ding C, Ma Y, Liu M, Zhang HG, Zheng J, Xiong N *et al* (2014) Differential developmental requirement and peripheral regulation for dermal Vγ4 and Vγ6T17 cells in health and inflammation. *Nat Commun* 5: 3986
49. Boyden LM, Lewis JM, Barbee SD, Bas A, Girardi M, Hayday AC, Tigelaar RE, Lifton RP (2008) Skint1, the prototype of a newly identified immunoglobulin superfamily gene cluster, positively selects epidermal γδT cells. *Nat Genet* 40: 656 – 662
50. Barbee SD, Woodward MJ, Turchinovich G, Mention JJ, Lewis JM, Boyden LM, Lifton RP, Tigelaar R, Hayday AC (2011) Skint-1 is a highly specific,

unique selecting component for epidermal T cells. *Proc Natl Acad Sci USA* 108: 3330 – 3335

51. Jensen KDC, Su X, Shin S, Li L, Youssef S, Yarnasaki S, Steinman L, Saito T, Locksley RM, Davis MM *et al* (2008) Thymic selection determines γδ cell effector fate: antigen-naive cells make Interleukin-17 and antigen-experienced cells make interferon γ. *Immunity* 29: 90 – 100
52. Reinhardt A, Ravens S, Fleige H, Haas JD, Oberdörfer L, Łyszkiewicz M, Förster R, Prinz I (2014) CCR7-mediated migration in the thymus controls γδ T-cell development. *Eur J Immunol* 44: 1320 – 1329
53. Hogquist KA, Jameson SC, Heath WR, Howard JL, Bevan MJ, Carbone FR (1994) T-cell receptor antagonist peptides induce positive selection. *Cell* 76: 17 – 27
54. Barnden MJ, Allison J, Heath WR, Carbone FR (1998) Defective TCR expression in transgenic mice constructed using cDNA-based alpha- and beta-chain genes under the control of heterologous regulatory elements. *Immunol Cell Biol* 76: 34 – 40
55. Shinkai Y, Rathbun G, Lam KP, Oltz EM, Stewart V, Mendelsohn M, Charron J, Datta M, Young F, Stall AM *et al* (1992) RAG-2-deficient mice lack mature lymphocytes owing to inability to initiate V(D)J rearrangement. *Cell* 68: 855 – 867
56. Cosgrove D, Gray D, Dierich A, Kaufman J, Lemeur M, Benoist C, Mathis D (1991) Mice lacking MHC class-II molecules. *Cell* 66: 1051 – 1066
57. Koller BH, Marrack P, Kappler JW, Smithies O (1990) Normal development of mice deficient in beta-2-m, MHC class I proteins, and $CD8^+$ T-cells. *Science* 248: 1227 – 1230
58. Mizuno A, Kanno T, Hoshi M, Shibata O, Yano K, Fujise N, Kinosaki M, Yamaguchi K, Tsuda E, Murakami A *et al* (2002) Transgenic mice over-expressing soluble osteoclast differentiation factor (sODF) exhibit severe osteoporosis. *J Bone Miner Metab* 20: 337 – 344
59. Oda H, Tamehiro N, Patrick MS, Hayakawa K, Suzuki H (2013) Differential requirement for RhoH in development of TCRαβ CD8αα IELs and other types of T cells. *Immunol Lett* 151: 1 – 9
60. Gray DHD, Chidgey AP, Boyd RL (2002) Analysis of thymic stromal cell populations using flow cytometry. *J Immunol Methods* 260: 15 – 28
61. Roark CL, Aydintug MK, Lewis J, Yin X, Lahn M, Hahn YS, Born WK, Tigelaar RE, O'Brien RL (2004) Subset-specific, uniform activation among Vγ6/Vδ1(+) γδT cells elicited by inflammation. *J Leukoc Biol* 75: 68 – 75
62. Nitta T, Ohigashi I, Takahama Y (2013) The development of T lymphocytes in fetal thymus organ culture. *Methods Mol Biol* 946: 85 – 102
63. Wang H, Yang H, Shivalila CS, Dawlaty MM, Cheng AW, Zhang F, Jaenisch R (2013) One-step generation of mice carrying mutations in multiple genes by CRISPR/Cas-mediated genome engineering. *Cell* 153: 910 – 918
64. Takeo T, Kaneko T, Haruguchi Y, Fukumoto K, Machida H, Koga M, Nakagawa Y, Takeshita Y, Matsuguma T, Tsuchiyama S *et al* (2009) Birth of mice from vitrified/warmed 2-cell embryos transported at a cold temperature. *Cryobiology* 58: 196 – 202
65. Fehling HJ, Swat W, Laplace C, Kuhn R, Rajewsky K, Muller U, Vonboehmer H (1994) MHC class-I expression in mice lacking the proteasome subunit LMP-7. *Science* 265: 1234 – 1237
66. Saitoh T, Nakano H, Yamamoto N, Yamaoka S (2002) Lymphotoxin-β receptor mediates NEMO-independent NF-κB activation. *FEBS Lett* 532: 45 – 51
67. Hirano Y, Kaneko T, Okamoto K, Bai M, Yashiroda H, Furuyama K, Kato K, Tanaka K, Murata S (2008) Dissecting β-ring assembly pathway of the mammalian 20S proteasome. *EMBO J* 27: 2204 – 2213
68. Ishikawa E, Ishikawa T, Morita YS, Toyonaga K, Yamada H, Takeuchi O, Kinoshita T, Akira S, Yoshikai Y, Yamasaki S (2009) Direct recognition of the mycobacterial glycolipid, trehalose dimycolate, by C-type lectin Mincle. *J Exp Med* 206: 2879 – 2888
69. Perez RL, Roman J, Staton GW, Hunter RL (1994) Extravascular coagulation and fibrinolysis in murine lung inflammation-induced by the mycobacterial cord factor trehalose-6,6′-dimycolate. *Am J Respir Crit Care Med* 149: 510 – 518